

1 Radio signals from electron beams in Terrestrial
2 Gamma-ray Flashes

Valerie Connaughton,^{1,2} Michael S. Briggs,^{1,2} Shaolin Xiong,¹ Joseph R.
Dwyer,³ Michael L. Hutchins,⁴ J. Eric Grove,⁵ Alexandre Chekhtman,⁶
Dave Tierney,⁷ Gerard Fitzpatrick,⁷ Suzanne Foley,⁷ Shelia McBreen,⁷
P. N. Bhat,¹ Vandiver L. Chaplin,¹ Eric Cramer,³ Gerald J. Fishman,⁸
Robert H. Holzworth,⁴ Melissa Gibby,⁸ Andreas von Kienlin,⁹
Charles A. Meegan,¹⁰ William S. Paciasas,¹⁰ Robert D. Preece,^{1,2} and
Colleen Wilson-Hodge.¹¹

3 **Abstract.** We show that the rate of association between Terrestrial Gamma-
4 ray Flashes (TGFs) observed by the Fermi Gamma-ray Burst Monitor (GBM)

P. N. Bhat, M. S. Briggs, V. Chaplin, V. Connaughton, R. D. Preece, and S. Xiong, CSPAR,
320 Sparkman Drive, Huntsville, AL, 35805, USA. (valerie@nasa.gov).

J. R. Dwyer and E. Cramer, Physics and Space Sciences, Florida Institute of Technology,
Melbourne, FL 32901, USA. (jdwyer@fit.edu)

R. H. Holzworth and M. L. Hutchins, Earth and Space Sciences, University of Washington,
Seattle, WA 98195, USA. (bobholz@ess.washington.edu)

G. Fitzpatrick, Suzanne Foley, S. McBreen and D. Tierney, School of Physics, University
College Dublin, Belfield, Dublin 4, Ireland. (sheila.mcbreen@ucd.ie)

A. Chekhtman and J. E. Grove, Space Science Division, U. S. Naval Research Laboratory,
Washington, D.C., 20375, USA. (eric.grove@nrl.navy.mil)

G. J. Fishman and M. Gibby, Jacobs Engineering Group Inc., 1500 Perimeter Parkway,
Huntsville, AL 35806, USA. (jerry.fishman@nasa.gov)

A. von Kienlin, Max-Planck Institut für extraterrestrische Physik, D-85741 Garching, Germany.
(azk@mpe.mpg.de)

C. A. Meegan and W. S. Paciesas, USRA, 320 Sparkman Drive, Huntsville, AL, 35805, USA.
(chip.meegan@nasa.gov).

C. Wilson-Hodge, Space Science Office, VP62, NASA Marshall Space Flight Center, Huntsville,
AL, 35812, USA. (Colleen.Wilson@nasa.gov)

¹CSPAR, University of Alabama in

5 and Very-Low Frequency (VLF) discharges detected by the World Wide Light-
6 ning Location Network (WWLLN) depends strongly on the duration of the
7 TGF, with the shortest TGFs having associated WWLLN events over 50%
8 of the time, and the longest TGFs showing a less than 10% match rate. This
9 correlation is stronger if one excludes the WWLLN discharges that are not
10 simultaneous (within $200 \mu\text{s}$) with the TGF. We infer that the simultaneous
11 VLF discharges are from the relativistic electron avalanches that are respon-
12 sible for the flash of gamma rays and the non-simultaneous VLF discharges
13 are from related Intra-Cloud lightning strokes. The distributions of far-field
14 radiated VLF stroke energy measured by WWLLN for the simultaneous and
15 non-simultaneous discharges support the hypothesis of two discrete popu-
16 lations of VLF signals associated with TGFs, with the simultaneous discharges
17 among the strongest measured by WWLLN.

Huntsville, Huntsville, AL, 35899, USA

1. Introduction

18 Terrestrial Gamma-ray Flashes (TGFs) are brief bursts of high-energy radiation discov-
19 ered by the Burst And Transient Source Experiment (BATSE) [*Fishman et al.*, 1994], and
20 detected since then by several high-energy satellite detectors: the Reuven Ramati High
21 Energy Solar Spectroscopic Imager (RHESSI) [*Smith et al.*, 2005; *Grefenstette et al.*,
22 2009; *Gjesteland et al.*, 2012], the Astrorivelatore Gamma a Immagini Leggero (AGILE)
23 [*Marisaldi et al.*, 2010a; *Fuschino et al.*, 2009; *Marisaldi et al.*, 2010b], and most re-
24 cently by the Gamma-ray Burst Monitor (GBM) on-board the Fermi Satellite [*Briggs*
25 *et al.*, 2010; *Fishman et al.*, 2011]. Their connection to lightning was suspected since
26 their discovery as the first detections occurred in satellites overflying regions with active
27 thunderstorms. TGFs are believed to originate in the large-scale electric fields near the
28 tops of thunderclouds and likely involve the acceleration and multiplication of electrons
29 emitting bremsstrahlung radiation and eventually discharging the field. Ground-based
30 networks detecting the Ultra-Low or Very-Low Frequency (ULF or VLF) radio signals
31 from electric field discharges found in coincidence with TGFs have been used to locate
32 the sources of TGFs to a small region within the larger footprint of the satellite over
33 the Earth. Correlations in time between electric field discharges and TGFs suggested a
34 temporal separation of no more than a few milliseconds [*Inan et al.*, 1996; *Cummer et al.*,
35 2005; *Stanley et al.*, 2006; *Inan et al.*, 2006; *Lay*, 2008; *Cohen et al.*, 2006, 2010] with more
36 precise relative timing hindered by a ~ 2 ms uncertainty in RHESSI timing and limita-

²Dept. of Physics, University of Alabama

37 tions of the BATSE-era radio networks. Using the timing accuracy of Fermi GBM and the
38 World Wide Lightning Location Network (WWLLN) [Rodger *et al.*, 2009], Connaughton
39 *et al.* [2010] showed that 15 of the first 50 TGFs that triggered GBM were associated with
40 a WWLLN-measured discharge, and that most of these discharges occurred near the time
41 of a TGF pulse peak. Of these associations within 5 ms of a TGF peak, 13 occurred within
42 tens of μ s of the peak, with one WWLLN discharge each between 1 and 5 ms either side
43 of the peak. The sample of GBM TGFs has greatly increased in size from the 50 events
44 reported in Connaughton *et al.* [2010]. In addition to 130 additional triggered TGFs, a
45 new data taking mode has been implemented whereby individual time-tagged photons
46 are downlinked when Fermi passes over regions of expected thunderstorm activity. These
47 regions are predefined and modified seasonally according to weather patterns. TGFs can
48 then be found on the ground in an offline search, rather than having to trigger on-board
49 in a 16 ms window wherein only the brightest TGFs are visible above threshold [Briggs
50 *et al.*, 2012]. We explore here the correlation between WWLLN-measured discharges and
51 a population of 601 TGF pulses that were detected between 08 August 2008 and 30 Au-
52 gust 2011, of which 180 were triggered TGFs (192 pulses) and 409 were uncovered using
53 the offline search. In addition to the 384 TGFs from the offline search [Briggs *et al.*, 2012],
54 of which three had two peaks that are counted separately, 22 TGFs were found outside
55 the time period or geographic region reported in that work, mostly in the time-tagged
56 event data surrounding triggered TGFs.

in Huntsville, Huntsville, AL, 35899, USA

2. Results

57 Guided by prior TGF-radio correlation results, we defined three search radii: (i) 300
58 km, identified in *Connaughton et al.* [2010] as the horizon for all the WWLLN discharges
59 associated with 15 triggered TGFs, (ii) 600 km radius as used in *Hazelton et al.* [2009]
60 and *Cohen et al.* [2010] to contain associations between RHESSI-detected TGFs and radio
61 signals, and (iii) 1000 km, as a more speculative choice to explore the possibility that,
62 with the offline search, GBM might be sensitive to weaker events from a larger distance.
63 Likewise, the 5 ms window defining an association with radio signals in both RHESSI and
64 GBM searches so far was retained, but two new windows (10 and 20 ms) were introduced
65 because the small number of TGFs found in *Connaughton et al.* [2010] that were associated
66 but not simultaneous with the TGF (i.e., not within $\pm 40 \mu\text{s}$) did not delineate a clear time
67 boundary either side of the TGF for determining statistically significant associations. We
68 calculate the probability of each association being a coincidence by finding the number of
69 matches in the WWLLN data of 1000 proxy TGF times at 1 s intervals within ± 500 s of
70 the TGF trigger time [*Connaughton et al.*, 2010]. We treat each time window and horizon
71 as a separate control sample for the purpose of determining the chance probability of each
72 match given the clustering of WWLLN events on the relevant timescale and geographical
73 region. A chance probability of more than 1% - 10 matches in the control sample - was
74 used to dismiss an association as a possible coincidence. In the sample of 601 TGFs,
75 198 produced WWLLN matches in one or more of the windows described above. Twelve
76 of these were rejected using an unacceptably high match rate in the control sample, of

³Physics and Space Sciences, Florida

77 which three were within the 5 ms window, and six beyond the 10 ms window. Of the
 78 186 significant matches, 182 were found within the 5 ms coincidence window. Three of
 79 the remaining four were found in the 5 - 10 ms window, with only one in the 10 - 20 ms
 80 window, suggesting that expanding the time window does not reveal many TGF/WWLLN
 81 associations, and those that are found in the expanded window have a high probability of
 82 occurring by chance.

83 Because the TGFs uncovered in the offline GBM search are weaker and have limited
 84 counting statistics, the pulse-fitting technique described in *Briggs et al.* [2010] and em-
 85 ployed in *Connaughton et al.* [2010] to establish the TGF peak time becomes difficult.
 86 Instead, we take the center of the T_{50} period, i.e., the period during which 50% of the
 87 total TGF fluence is observed, starting from the 25% fluence level time [*Fishman et al.*,
 88 2011]. The peak is not located as precisely using this method as with the pulse-fitting
 89 algorithm, and we reestablish our definition of GBM-WWLLN simultaneity by examining
 90 the temporal offsets between the WWLLN discharge times of group arrival and the TGF
 91 T_{50} center times, corrected for light travel time to Fermi, shown in Figure 1. The $\pm 40 \mu\text{s}$
 92 envelope for simultaneity established in *Connaughton et al.* [2010] is expanded to $\pm 200 \mu\text{s}$.
 93 This $400 \mu\text{s}$ interval centered on the mid-point of the T_{50} is well-matched to the typical
 94 duration of a TGF, which we characterize by T_{90} , the 5% to 95% fluence accumulation
 95 period [*Briggs et al.*, 2012]. Although the T_{50} interval contains only 50% of the TGF
 96 fluence, we adopt it here as a more robust measure of duration compared to T_{90} because
 97 it is less susceptible to uncertainties caused by low count rates and background counts
 98 in the tail of the TGF. Using these definitions, 154 of the 186 WWLLN discharges are

Institute of Technology, Melbourne, FL

99 simultaneous with the gamma-ray peak of the TGF. No WWLLN discharges simultaneous
100 with the TGF had enough matches in the control samples to cause their rejection as real
101 associations.

102 In contrast to the expanded time windows, the expanded search radii revealed many
103 WWLLN matches, particularly among the TGFs found offline, but even some of the
104 triggered TGFs occurred beyond the 300 km horizon established in *Connaughton et al.*
105 [2010]. The most distant association that passed the control sample test was 954 km
106 from the Fermi nadir. The spacecraft was flying over Madagascar, and examination of
107 the WWLLN lightning map during the 20 minutes surrounding the TGF reveals storm
108 systems that are closer to the spacecraft nadir and more credible as the source of the
109 TGF. The angular offset distribution of TGFs is shown in Figure 7 of *Briggs et al.* [2012]
110 to decline beyond 300 km and tail off smoothly by 800 km. We cannot dismiss the more
111 distant match using our established rejection criteria, but the fact that the second farthest
112 WWLLN discharge associated with a TGF is 200 km closer to the nadir suggests that
113 this 954 km match may be a false positive. Based on this reasoning, we consider the
114 maximum horizon for a WWLLN discharge to be a credible association with a GBM
115 TGF to be around 800 km. An all-sky search for matches revealed eight beyond the 1000
116 km limit of this analysis, all of which produced unacceptable chance coincidences in the
117 control samples, and all but one of them outside the 5 ms time window. This suggests
118 that one needs to worry about false associations using the WWLLN data when searching
119 at large source distance and temporal offsets in the expanded time windows but that the

32901, USA

120 results of our search within the narrow time window and up to eight hundred km search
121 radius are reliable.

122 The match rate in the population of TGFS that triggered GBM (26%) is lower than in
123 the offline search sample (33%), meaning that the TGFS that show fewer counts in the
124 GBM detectors are more likely to be associated with a discharge measured by WWLLN,
125 a result that seems puzzling if one considers that for a given intrinsic TGF intensity the
126 number of counts detected by GBM depends only on the TGF-Fermi geometry. The mea-
127 sured intensity is inversely proportional to the square of the source distance from Fermi
128 for a given angular offset, and is strongly influenced by atmospheric attenuation. For
129 TGFS viewed at larger angular offsets, the measured flux is lower when Fermi measures
130 scattered flux outside the direct beam [Østgaard *et al.*, 2008; Hazelton *et al.*, 2009; Col-
131 lier *et al.*, 2011; Gjesteland *et al.*, 2011]. These factors should not affect the likelihood
132 of the associated discharge being measured by WWLLN. A Kolmogorov-Smirnov (KS)
133 test of the T_{50} count fluence distributions of the 186 and 408 TGFS with and without
134 associated WWLLN discharges gives a probability of 0.09 that they are drawn from the
135 same population, with this probability decreasing to 0.07 if one considers only the 154
136 TGFS with simultaneous WWLLN discharges. This is suggestive of a correlation between
137 TGF fluence and the detection of an associated discharge by WWLLN, a link that was
138 also noted by Collier *et al.* [2011] and Gjesteland *et al.* [2012] in an analysis of RHESSI
139 TGFS and WWLLN events. While the statistical significance of the match rate versus
140 gamma-ray counts is modest in the GBM sample, the prior detection of this correlation

⁴Earth and Space Sciences, University of

141 in an independent sample indicates that it is not due to chance. We find, however, a
142 more striking correlation when instead of comparing the fluence distributions of the sam-
143 ples of TGFs with and without associated WWLLN discharges, we compare the duration

Washington, Seattle, WA 98195, USA

⁵Space Science Division, U. S. Naval
Research Laboratory, Washington, D.C.,
20375, USA

⁶George Mason University, Fairfax, VA,
22030, USA

⁷University College Dublin, Belfield,
Dublin 4, Ireland

⁸Jacobs Engineering Group Inc.,
Huntsville, AL 35806, USA.

⁹Max-Planck Institut für
extraterrestrische Physik, D-85741
Garching, Germany

¹⁰Universities Space Research Association,
Huntsville, AL, 35803, USA

¹¹Space Science Office, NASA Marshall
Space Flight Center, Huntsville, AL, 35812,
USA

144 distributions of these two samples. This comparison yields a KS probability of 10^{-12}
145 that the T_{50} distributions of the TGFS with and without WWLLN associations are drawn
146 from the same population, decreasing to 10^{-16} if we restrict the sample with WWLLN
147 matches to the 154 TGFS with simultaneous WWLLN discharges. These T_{50} distributions
148 are displayed in Figure 2 (top panel), which also illustrates that the rate of association
149 between TGFS and WWLLN discharges increases steadily with decreasing TGF duration
150 (lower panel). A Spearman's rank-order correlation of -0.97 is found for the WWLLN
151 match-rate fraction as a function of T_{50} , corresponding to a probability of 2×10^{-5} that
152 this correlation occurred by chance. This relation is even tighter if we exclude the 32
153 TGFS for which the WWLLN discharge is not simultaneous with the TGF, indicating
154 a near-perfect anti-correlation between the durations of TGFS and the detection rate of
155 associated simultaneous discharges by WWLLN.

3. Discussion

156 We have established that the TGFS detected using GBM show an approximately 30%
157 rate of associations with discharges measured by WWLLN, down to the weakest TGFS
158 detected so far, and that this association rate varies according to the duration of the TGF.
159 Using the National Lightning Detection Network (NLDN) as ground truth, the efficiency
160 for lightning detection of WWLLN over the US was estimated to be around 10% in 2008
161 for Cloud-to-Ground lightning when GBM began operations [*Abarca et al.*, 2010] with
162 lower efficiencies outside the US and Caribbean [*Hutchins et al.*, 2012a]. This efficiency
163 has improved with the addition of new receiving stations and the development of more
164 sophisticated signal processing algorithms [*Rodger et al.*, 2009], but it is imperfect, limited
165 by the size of the discharge that is measured at multiple stations and triangulated at the

166 time of its estimated peak power, and varies according to changing ionospheric conditions
167 (day-night effects), differences in VLF propagation over land, oceans, and ice, and the
168 presence of local lightning activity, which raises the detection threshold for more distant
169 strokes [*Hutchins et al.*, 2012a]. According to the detection efficiency calculations of *Abarca*
170 *et al.* [2010], our association rate of 30% suggests that if discharges seen in association with
171 TGFs are attributable to lightning, then they have unusually high currents, and that the
172 shorter TGFs are associated with the strongest discharges measured by WWLLN. Using
173 the match rates from Figure 2 one can use the WWLLN stroke detection efficiency as a
174 function of peak current presented in Figure 3 of *Abarca et al.* [2010] to infer an average
175 peak current for each T_{50} time bin. TGFs longer than 210 μs are associated with currents
176 below 10 kA, those lasting from 90 to 210 μs range from 80 kA to 35 kA, and the shortest
177 TGFs with a greater than 50% match rate are associated with currents above 150 kA.
178 This suggests a puzzling dependence on TGF duration of the current from the associated
179 lightning discharge.

180 If instead of lightning, WWLLN is detecting the TGF itself [*Cummer et al.*, 2011;
181 *Dwyer*, 2012], then a relationship between the characteristics of the TGF and its de-
182 tectability by WWLLN is more natural. Let us consider the electrical currents and the
183 resulting radio frequency emissions that are generated by the runaway electron avalanches
184 that compose the TGF. Here, we do not include any electrical currents that might be di-
185 rectly made by the lightning processes [*Carlson et al.*, 2010]. As the runaway electrons
186 propagate, they ionize the air, creating low-energy (few eV) electrons and ions that drift
187 in the electric field. Most of the electrical current generated by the runaway electron
188 avalanches comes from the drifting low-energy electrons. Because these low-energy elec-

189 trons quickly attach to oxygen atoms, usually on a time scale less than a few μs , the
 190 electrical current generated by the TGF will closely follow the time-structure of the TGF
 191 gamma rays at the source. At spacecraft altitudes the duration of the TGF may be in-
 192 creased due to Compton scattering in the atmosphere [*Østgaard et al.*, 2008; *Grefenstette*
 193 *et al.*, 2008; *Gjesteland et al.*, 2010]. However, the higher energy photons (> 1 MeV) will
 194 most closely match the original duration of the TGF at the source, since these photons
 195 will have undergone the least Compton scattering.

196 Following *Dwyer* [2012] we consider a rate of runaway electrons [number per sec] that
 197 follows a Gaussian distribution in time with RMS, σ . For a Gaussian distribution, $\sigma =$
 198 $0.74T_{50}$. The current moment as a function of time is then

$$I_{mom} = \frac{e\alpha\tau_a\mu_e EN_{re}\Delta z}{\sqrt{2\pi}0.74T_{50}} \exp\left(\frac{-t^2}{2(0.74T_{50})^2}\right) \quad (1)$$

199 where e is the charge of the electron; α is the ionization per unit length per runaway
 200 electron; μ_e is the mobility of the low-energy electrons, τ_a their attachment time; E is
 201 the electric field strength; N_{re} is the total number of runaway electrons; and Δz is the
 202 vertical distance over which the runaway electrons travel [*Dwyer*, 2012]. From RHESSI
 203 observations, at an altitude of 13 km, the combination $N_{re}\Delta z = 1.5 \times 10^{20}$ m [*Dwyer and*
 204 *Smith*, 2005; *Dwyer*, 2012]. At 13 km, $\tau_a = 1.3 \times 10^{-6}$ s, $\mu_e = 0.4 \text{ m}^2/\text{Vs}$ [*Morrow and*
 205 *Lowke*, 1997; *Liu and Pasko*, 2004] and $\alpha = 1,900 \text{ m}^{-1}$ (scaled from a sea-level value of
 206 $8,350 \text{ m}^{-1}$) [*Dwyer and Babich*, 2011]. Finally, most of the runaway electrons are produced
 207 at the end of the avalanche region where $E = 2.84 \times 10^5 \text{ V/m} \times n = 6.4 \times 10^4 \text{ V/m}$, where
 208 n is the density of air relative to sea level.

209 As can be seen from Eq. 1, for the same number of runaway electrons and hence the
 210 same number of gamma rays emitted at the source, a shorter TGF produces a larger peak
 211 current moment. Furthermore, a shorter TGF emits more radio frequency (RF) energy
 212 at higher frequencies, which is important when considering the frequency threshold of
 213 WWLLN (> 6 kHz).

214 At large horizontal distances, the radiation electric field emitted by the current moment,
 215 I , in Eq. 1 is given by

$$E_{rad} = \frac{\sin \theta}{4\pi\epsilon_0 c^2 R} \frac{\partial I}{\partial t} \quad (2)$$

216 where all the symbols have their usual meaning [Uman, 2001]. Inserting Eq. 1 into Eq. 2
 217 and taking the Fourier transform gives

$$E(\omega) = -i\omega \frac{e\alpha\tau_a\mu_e EN_{re}\Delta z \sin \theta}{\sqrt{2\pi}4\pi\epsilon_0 c^2 R} \exp\left(\frac{-\omega^2(0.74T_{50})^2}{2}\right) \quad (3)$$

218 where ω is the angular frequency. The spectral energy density (energy radiated per unit
 219 frequency) is proportional to the square of Eq. 3.

220 WWLLN was optimized for measuring lightning, which has peak spectral energy density
 221 around 10 kHz. Its detectors record the RF signal from 1 to 24 kHz, with data between 6
 222 and 18 kHz contributing to the nominal analysis. *Jacobson et al.* [2006] found a significant
 223 fraction of intra-cloud (IC) lightning discharges correlated with very short duration (\sim
 224 $20 \mu\text{s}$) Narrow Bipolar Events detected by the Los Alamos Sferic Array, suggesting a high
 225 WWLLN efficiency for detecting powerful short events. From Eq. 3, the TGF will also
 226 produce an RF signal with a peak spectral energy density at 10 kHz, similar to lightning,

227 when $T_{50} = 21.5 \mu\text{s}$. In this case, the peak current moment (Eq. 1) is 40 kA-km. If
 228 we assume that $\Delta z \sim 1$ km, then the peak current in this case is 40 kA, a large value,
 229 comparable to lightning. Therefore, it is expected that the WWLLN would efficiently
 230 detect such short TGFs.

231 On the other hand, as can be seen in Eq. 3, the energy radiated into the WWLLN
 232 detection band falls very quickly as T_{50} increases. For example, for $T_{50} = 150 \mu\text{s}$, the
 233 energy radiated into the 6 - 18 kHz band is 6×10^7 times smaller than the energy radiated
 234 into that band when $T_{50} = 50 \mu\text{s}$ [Hutchins *et al.*, 2012a]. From Eq. 1 we would expect
 235 the detection efficiency to decrease greatly with increased T_{50} values, but the observed
 236 decrease (Figure 2) is much more gradual than expected from Eq. 3.

237 We consider several explanations to explain the WWLLN efficiency for longer TGFs
 238 being higher than expected in our simple model. First, there could be additional light-
 239 ning currents during many TGFs that, when added to the currents from the TGF itself,
 240 combine to put the event over the WWLLN detection threshold for longer TGFs. Second,
 241 a TGF arising deeper in the atmosphere than the 13 km assumed in Eq 1 will yield more
 242 electrons and a higher current, since more runaway electrons are needed to produce the
 243 same fluence of gamma rays exiting the atmosphere. Third, our characterization of TGF
 244 duration is subject to observational and instrumental effects. Longer TGFs may contain
 245 substructure (shorter current pulses) that efficiently radiate in the WWLLN frequency
 246 band. Briggs *et al.* [2010] show that in addition to multi-pulse TGFs that we consider
 247 here on a per-pulse basis, some TGFs are likely a superposition of shorter pulses (see
 248 also Celestin and Pasko [2012]), and that some pulses are Gaussian and others are better
 249 fit using a log normal function that can have a very fast rise time, as short as $7 \mu\text{s}$. In

250 general, our assumption regarding the Gaussian shape of a TGF gives a rather pessimistic
251 prediction for WWLLN detection, and a sharper rise or decay will yield more energy at
252 higher frequencies. For some TGFs, Compton scattering may make the duration of the
253 gamma-ray flash measured by GBM significantly longer than the duration of the electron
254 avalanche. Some of the long TGFs, then, might be efficiently detected by WWLLN, while
255 others might be intrinsically long and do not produce enough RF energy in the WWLLN
256 band to be detected. The T_{50} values in Figure 2 are measured over the entire energy
257 range seen by GBM (8 keV - 40 MeV). If we restrict the T_{50} calculation to energies above
258 300 keV, we can see from Figure 3 that the number of shorter TGFs with associated
259 WWLLN discharges is higher and the rate of longer TGFs with WWLLN matches lower,
260 an effect that is not seen in the TGF population without WWLLN matches. Owing to
261 poor statistics, the T_{50} measurement becomes difficult when the energy range is further
262 restricted, but the fact that longer events with WWLLN matches appear shorter at higher
263 energies supports the hypothesis that their duration is lengthened by Compton scattering
264 on the way to Fermi. A final instrumental effect concerns the deadtime suffered in the
265 GBM detectors. One effect of deadtime is to underestimate the intensity at the peak of
266 the TGF, thus artificially lengthening the T_{50} estimate. The effect of deadtime can also
267 explain the higher match rate of the population of TGFs from the offline search if we
268 consider a population of TGFs, all with about the same fluence of gamma rays at the
269 source, but with a distribution of durations. In this population, the ones that are most
270 likely to have a match are the very short ones (keeping in mind that they may appear
271 longer in GBM due to Compton scattering and deadtime). Because of dead time, the
272 number of photons detected by GBM should always be less for shorter TGFs. Therefore

273 when the fluence (total numbers of counts) threshold of a GBM TGF sample is lowered,
274 the proportion of short TGFs will increase, causing the WWLLN match rate of the sample
275 to increase. Both effects are seen in the offline search sample of *Briggs et al.* [2012], and
276 this reasoning can also explain the result from *Collier et al.* [2011] and *Gjesteland et al.*
277 [2012] that the weaker RHESSI TGFs have a higher WWLLN association rate. It is not
278 the weakness of the TGF that makes it more likely to have a WWLLN association but
279 its shortness: a short TGF is more likely to have fewer counts than a longer TGF.

280 The combination of instrumental effects (deadtime), source behavior (Compton scat-
281 tering, overlapping pulses, non-Gaussian shapes, fast risetimes), and model assumptions
282 (contributions to current from lightning, source height) complicates the relationship be-
283 tween WWLLN detection rate and TGF duration, although it is qualitatively as one would
284 expect if the TGF is responsible for the radio signal. Given the close relationship expected
285 between the RF signal and the gamma-ray time profile, only the simultaneous associations
286 can be attributed to the TGF itself. The WWLLN associations that are not simultaneous
287 (greater than $\pm 200 \mu\text{s}$ from the TGF peak) but still significantly temporally and spatially
288 coincident with the TGF could then be discharges from regular IC lightning activity that
289 is also believed to be associated with TGFs [*Stanley et al.*, 2006; *Lu et al.*, 2010]. The
290 time boundary between simultaneous and non-simultaneous is ill-defined. Indeed, if the
291 non-simultaneous associations occur non-preferentially with respect to the time of the
292 TGF, as suggested by the distribution in Figure 1, then given the number of matches 5
293 ms either side of the TGF, one might expect from Poisson statistics that between one
294 and three of the simultaneous matches are actually part of the lightning-related sample
295 rather than due to the TGF. If the lightning-related events that are mis-classified as TGF

296 emission are associated with longer TGFS, this further contributes to the match rate of
297 longer TGFS being higher than expected from Relativistic Runaway Electron Avalanche
298 (RREA) theory. Only 32 TGFS have non-simultaneous matches outside the window for
299 simultaneity, and removing them from the sample of TGFS associated with WWLLN dis-
300 charges tightens the anti-correlation between match rate and TGF duration, from which
301 one can also conclude there is no correlation between the non-simultaneous match rate
302 and TGF duration. These 32 associations from a total sample of 601 TGFS suggest a
303 detection efficiency of 5% for the IC lightning associated with TGFS. This is consistent
304 with the estimates of *Abarca et al.* [2010] of 4.5% detection efficiency of WWLLN for IC
305 lightning with peak currents greater than 15 kA. One TGF in our sample has both a
306 simultaneous and a non-simultaneous association with WWLLN. The geolocations are 20
307 km apart, so a common origin is possible given the localization uncertainty of WWLLN
308 [*Hutchins et al.*, 2012a]. If each TGF has both a simultaneous discharge and one associ-
309 ated with IC lightning that may not be simultaneous, then one might expect WWLLN
310 to detect the IC lightning for the 154 TGFS it detected directly 5% of the time, giving
311 seven or eight TGFS where both discharges are detected by WWLLN, yet we have only
312 one such case. Two factors may explain this: each WWLLN station has a deadtime of
313 ~ 1.3 ms following a detection, so that a smaller number of stations can detect the second
314 discharge and the probability of detecting both discharges is reduced. The effect is prob-
315 ably more severe for the case where the TGF occurs first, given that the discharge with
316 the higher-power TGF will incapacitate more stations than the lower-power IC discharge.
317 The simultaneous and non-simultaneous discharges might also be mis-identified as dupli-
318 cate measurements of the same discharge, a possibility that arises because it is common to

319 make multiple measurements of a single discharge with different combinations of WWLLN
320 stations and to remove the duplicate event manually. The factors leading the removal of
321 duplicates are temporal coincidence (within 1 ms), common origin (20 km) and similar
322 power. The power measurements can be subject to large uncertainties [*Hutchins et al.*,
323 2012b] so that a simultaneous or non-simultaneous event with an ill-constrained power
324 measurement may have been mistakenly removed in this process, leading to a lower-than-
325 expected number of cases where both the TGF and the IC lightning were detected. The
326 match rate for the non-simultaneous discharges is consistent with estimated efficiencies
327 for WWLLN IC detection. Qualitatively the presence of one case where we detect both
328 the non-simultaneous and simultaneous discharges is consistent with our hypothesis of 2
329 types of discharges for each TGF. The number of cases where both types of discharge are
330 identified may be lower than expected because of network and processing inefficiencies for
331 discharges this close in time and space.

332 The hypothesis that two different types of VLF signal are associated with TGFs is
333 supported by differences in the characteristics of the radio signals of the two popula-
334 tions. Figure 4 shows that the median far-field radiated VLF stroke energy measured
335 by WWLLN for the simultaneous discharges is much higher (3.1 kJ) than for the non-
336 simultaneous discharges (700 J), with the latter typical of the median stroke energy for
337 WWLLN [*Hutchins et al.*, 2012b]. In measurements of the wave-forms of radio discharges
338 measured by the Duke telescopes in association with RHESSI-detected TGFs, *Lu et al.*
339 [2011] find two types of pulses, with a slow ULF pulse accompanying the TGF (within
340 the 2 ms timing uncertainty of RHESSI) and fast VLF pulses preceding the TGF. The
341 ULF waveform may be the counterpart to the simultaneous WWLLN match and the fast

342 VLF pulses akin to the non-simultaneous matches, but we note from Figure 1 that our
343 non-simultaneous matches do not show a preferred order, whereas the fast VLF pulses of
344 *Lu et al.* [2011] are all precursors to the TGF.

345 The identification of TGFs as the source of the radio emission in the simultaneous cases
346 explains the tightness of the simultaneity ($\pm 40 \mu\text{s}$) found by *Connaughton et al.* [2010]
347 and suggested in prior studies using RHESSI data [*Inan et al.*, 1996; *Cummer et al.*, 2005;
348 *Stanley et al.*, 2006; *Inan et al.*, 2006; *Lay*, 2008; *Cohen et al.*, 2006, 2010]. Our results
349 strongly suggest that two types of VLF radio signals are associated with TGFs: one, very
350 strong and simultaneous with the TGF, is the TGF itself; the other, weaker and occurring
351 up to several ms either side of the TGF, is a lightning event associated with the TGF.

352 **Acknowledgments.** The Fermi GBM Collaboration acknowledges support for GBM
353 development, operations, and data analysis from National Aeronautics and Space Admin-
354 istration (NASA) in the United States and from the Bundesministerium für Wirtschaft
355 und Technologie (BMWi) / Deutsches Zentrum für Luft und Raumfahrt (DLR) in Ger-
356 many. This work was supported in part by NASA’s Fermi Guest Investigator Program and
357 by DARPA grant HR0011-10-1-0061. D.T. acknowledges support from Science Foundation
358 Ireland under grant number 09-RFP-AST-2400. S.F. and G.F. acknowledge the support
359 of the Irish Research Council for Science, Engineering and Technology; S.F. is cofunded
360 by Marie Curie Actions under FP7. The authors wish to thank the World Wide Lightning
361 Location Network (<http://wwlln.net>), a collaboration among over 50 universities and in-
362 stitutions, for providing the lightning location data used in this paper. We appreciate
363 the freely-available Coyote resources for IDL programming, which helped generate all the

364 histograms in this paper (<http://www.idlcoyote.com/>). We thank Nikolai Østgaard and
365 an anonymous reviewer for helpful suggestions during the refereeing process.

References

- 366 Abarca, S. F., K. L. Corbosiero, and T. J. Galarneau, Jr (2010), An evaluation of
367 the worldwide lightning location network (WWLLN) using the national lightning
368 detection network (NLDN) as ground truth, *J. Geophys. Res.*, *115*, D18,206, doi:
369 10.1029/2009JD013411.
- 370 Briggs, M. S., G. J. Fishman, V. Connaughton, P. N. Bhat, W. S. Paciesas, R. D.
371 Preece, C. Wilson-Hodge, V. L. Chaplin, R. M. Kippen, A. von Kienlin, C. A. Meegan,
372 E. Bissaldi, J. R. Dwyer, D. M. Smith, R. H. Holzworth, J. E. Grove, and A. Chekhtman
373 (2010), First results on terrestrial gamma-ray flashes from the Fermi gamma-ray burst
374 monitor, *J. Geophys. Res.*, *115*, A07,323, doi:10.1029/2009JA015242.
- 375 Briggs, M. S., V. Connaughton, C. WilsonHodge, R. D. Preece, G. J. Fishman, R. M.
376 Kippen, P. N. Bhat, W. S. Paciesas, V. L. Chaplin, C. A. Meegan, A. von Kienlin,
377 J. Greiner, J. R. Dwyer, and D. M. Smith (2011), Electron-positron beams from ter-
378 restrial lightning observed with Fermi GBM, *Geophys. Res. Lett.*, *38*, L02,808, doi:
379 10.1029/2010GL046259.
- 380 Briggs, M. S., S. Xiong, V. Connaughton, D. Tierney, G. Fitzpatrick, S. Foley, E. Grove,
381 A. Chekhtman, M. Gibby, G. J. Fishman, S. McBreen, V. L. Chaplin, S. Guiriec,
382 E. Layden, P. N. Bhat, M. Hughes, J. Greiner, R. M. Kippen, C. A. Meegan, W. S.
383 Paciesas, R. D. Preece, A. von Kienlin, C. Wilson-Hodge, R. H. Holzworth, , and M. L.
384 Hutchins (2012), Terrestrial gamma-ray flashes in the fermi era: Improved observations

- 385 and analysis methods, *J. Geophys. Res.*, *0*, 0.
- 386 Carlson, B. E., N. G. Lehtinen, and U. S. Inan (2010), Terrestrial gamma ray flash
387 production by active lightning leader channels, *J. Geophys. Res.*, *115*, A10,324, doi:
388 10.1029/2010JA015647.
- 389 Celestin, S., and V. P. Pasko (2012), Compton scattering effects on the duration of terres-
390 trial gamma-ray flashes, *Geophys. Res. Lett.*, *39*, L02,802, doi:10.1029/2011GL050342.
- 391 Cohen, M. B., U. S. Inan, and G. Fishman (2006), Terrestrial gamma ray flashes ob-
392 served aboard the Compton gamma ray observatory/burst and transient source ex-
393 periment and ELV/VLF radio atmospherics, *J. Geophys. Res.*, *111*, D24,109, doi:
394 10.1029/2005JD006987.
- 395 Cohen, M. B., U. S. Inan, R. K. Said, and T. Gjestland (2010), Geolocation of terrestrial
396 gamma-ray flash source lightning, *Geophys. Res. Lett.*, *37*, doi:10.1029/2009GL041753.
- 397 Collier, A. B., T. Gjesteland, and N. Østgaard (2011), Assessing the power law distribution
398 of TGFs, *J. Geophys. Res.*, *116*, A10,320, doi:10.1029/2011JA016612.
- 399 Connaughton, V., M. S. Briggs, R. H. Holzworth, M. Hutchins, G. J. Fishman, C. A.
400 Wilson-Hodge, V. L. Chaplin, P. N. Bhat, J. Greiner, A. von Kienlin, R. M. Kippen,
401 C. A. Meegan, W. S. Paciesas, R. D. Preece, E. Cramer, J. R. Dwyer, , and D. M. Smith
402 (2010), Associations between Fermi GBM terrestrial gamma-ray flashes and sferics from
403 the WWLLN, *J. Geophys. Res.*, *115*, A12,307, doi:10.1029/2010JA015681.
- 404 Cummer, S. A., Y. Zhai, W. Hu, D. M. Smith, L. I. Lopez, and M. A. Stanley (2005),
405 Measurements and implications of the relationship between lightning and terrestrial
406 gamma ray flashes, *Geophys. Res. Lett.*, *32*, L08,811, doi:10.1029/2005GL022778.

- 407 Cummer, S. A., G. Lu, M. S. Briggs, V. Connaughton, S. Xion, G. J. Fishman, and J. R.
408 Dwyer (2011), The lightning-tgf relationship on microsecond timescales, *Geophys. Res.*
409 *Lett.*, *38*, L14,810, doi:10.1029/2011GL048099.
- 410 Dwyer, J. R. (2012), The relativistic feedback discharge model of terrestrial gamma ray
411 flashes, *J. Geophys. Res.*, *117*, A02,308, doi:10.1029/2011JA017160.
- 412 Dwyer, J. R., and L. Babich (2011), Low-energy electron production by relativis-
413 tic runaway electron avalanches in air, *J. Geophys. Res.*, *116*, A09,301, doi:
414 10.1029/2011JA016494.
- 415 Dwyer, J. R., and D. M. Smith (2005), A comparison between monte carlo simulations of
416 runaway breakdown and terrestrial gamma-ray flash observations, *Geophys. Res. Lett.*,
417 *32*, L22,804, doi:10.1029/2005GL023848.
- 418 Fishman, G. J., P. N. Bhat, R. Mallozzi, J. M. Horack, T. Koshut, C. Kouveliotou,
419 G. N. Pendleton, C. A. Meegan, R. B. Wilson, W. S. Paciesas, S. J. Goodman, and
420 H. J. Christian (1994), Discovery of intense gamma-ray flashes of atmospheric origin,
421 *Science*, *264*, 1313–1316.
- 422 Fishman, G. J., M. S. Briggs, V. Connaughton, P. N. Bhat, W. S. Paciesas, A. von Kienlin,
423 C. Wilson-Hodge, R. M. Kippen, R. Preece, C. A. Meegan, and J. Greiner (2011),
424 Temporal properties of terrestrial gamma-ray flashes from the gamma-ray burst monitor
425 on the Fermi observatory, *J. Geophys. Res.*, *116*, A07,304, doi:10.1029/2010JA016084.
- 426 Fuschino, F., F. Longo, M. Marisald, et al. (2009), AGILE view of TGFs, in *Conf. Proc.*
427 *1118, Coupling of Thunderstorms and Lightning Discharges to Near-Earth Space*, edited
428 by N. B. Crosby, T.-Y. Huang, and M. J. Rycroft, pp. 46–51, AIP.

- 429 Gjesteland, T., N. Østgaard, P. H. Connell, J. Stadsnes, and G. J. Fishman (2010),
430 Effects of dead time losses on terrestrial gamma ray flash measurements with
431 the Burst and Transient Source Experiment, *J. Geophys. Res.*, *115*, A00E21, doi:
432 10.1029/2009JA014578.
- 433 Gjesteland, T., N. Østgaard, A. B. Collier, B. E. Carlson, M. B. Cohen, and N. G. Lehtinen
434 (2011), Confining the angular distribution of terrestrial gamma ray flash emission, *J.*
435 *Geophys. Res.*, *116*, A11,313, doi:10.1029/2011JA016716.
- 436 Gjesteland, T., N. Østgaard, A. B. Collier, B. E. Carlson¹, C. Eyles, and D. M. Smith
437 (2012), A new method reveals more TGFs in the RHESSI data, *Geophys. Res. Lett.*,
438 doi:10.1029/2012GL050899.
- 439 Grefenstette, B. W., D. M. Smith, J. R. Dwyer, and G. J. Fishman (2008), Time
440 evolution of terrestrial gamma ray flashes, *Geophys. Res. Lett.*, *35*, L06,802, doi:
441 10.1029/2007GL032922.
- 442 Grefenstette, B. W., D. M. Smith, B. J. Hazelton, and L. I. Lopez (2009), First
443 RHESSI terrestrial gamma ray flash catalog, *J. Geophys. Res.*, *114*, A02,314, doi:
444 10.1029/2008JA013721.
- 445 Hazelton, B. J., B. W. Grefenstette, D. M. Smith, J. R. Dwyer, X.-M. Shao, S. A.
446 Cummer, T. Chronis, E. H. Lay, and R. H. Holzworth (2009), Spectral dependence
447 of terrestrial gamma-ray flashes on source distance, *Geophys. Res. Lett.*, *36*, L01,108,
448 doi:10.1029/2008GL035906.
- 449 Hutchins, M. L., R. H. Holzworth, J. B. Brundell, and C. J. Rodger (2012a), Relative
450 detection efficiency of the world wide lightning location network, *Radio Sci.*, *0*, 0.

- 451 Hutchins, M. L., R. H. Holzworth, C. J. Rodger, and J. B. Brundell (2012b), Far-field
452 power of lightning strokes as measured by the world wide lightning location network,
453 *J. Atmos. Oceanic Technol.*, *29*, 1102–1110.
- 454 Inan, U. S., S. C. Reising, G. J. Fishman, and J. M. Horack (1996), On the association of
455 terrestrial gamma-ray bursts with lightning and implications for sprites, *Geophys. Res.
456 Lett.*, *23*, 1017–1020.
- 457 Inan, U. S., M. B. Cohen, R. K. Said, D. M. Smith, and L. I. Lopez (2006), Terrestrial
458 gamma ray flashes and lightning discharges, *Geophys. Res. Lett.*, *33*, L18,802, doi:
459 10.1029/2006GL027085.
- 460 Jacobson, A. R., R. Holzworth, J. Harlin, R. Dowden, and E. Lay (2006), Performance
461 assessment of the world wide lightning location network (wwln), using the los alamos
462 spheric array (lasa) array as ground-truth, *J. Atmos. Oceanic Technol.*, *23*, 1082–92.
- 463 Lay, E. H. (2008), Investigating lightning-to-ionosphere energy coupling based on VLF
464 lightning propagation characterization, Ph.D. thesis, University of Washington.
- 465 Liu, N., and V. P. Pasko (2004), Effects of photoionization on propagation and branch-
466 ing of positive and negative streamers in sprites, *J. Geophys. Res.*, *109*, A04,301, doi:
467 10.1029/2003JA010064.
- 468 Lu, G., R. J. Blakeslee, J. Li, D. M. Smith, X.-M. Shao, E. W. McCaul, D. E.
469 Buechler, H. J. Christian, J. M. Hall, and S. A. Cummer (2010), Lightning map-
470 ping observation of a terrestrial gammaray flash, *Geophys. Res. Lett.*, *37*, L11,806,
471 doi:10.1029/2010GL043494.
- 472 Lu, G., S. A. Cummer, J. Li, F. Han, D. M. Smith, and B. W. Grefenstette (2011),
473 Characteristics of broadband lightning emissions associated with terrestrial gamma ray

- 474 flashes, *J. Geophys. Res.*, *116*, A03,316, doi:10.1029/2010JA016141.
- 475 Marisaldi, M., F. Fuschino, C. Labanti, M. Galli, F. Long, E. D. Monte, et al. (2010a),
476 Detection of terrestrial gamma-ray flashes up to 40 MeV by the AGILE satellite, *J.*
477 *Geophys. Res.*, *115*, A00E13, doi:10.1029/2009JA014502.
- 478 Marisaldi, M., A. Argan, A. Trois, A. Giuliani, M. Tavani, C. Labanti, F. Fuschino, et al.
479 (2010b), Gamma-ray localization of terrestrial gamma-ray flashes, *Phys. Rev. Lett.*, *105*,
480 128,501, doi:10.1103/PhysRevLett.105.128501.
- 481 Morrow, R., and J. J. Lowke (1997), Streamer propagation in air, *J. Phys. D: Appl. Phys.*,
482 *30*, 614–627.
- 483 Østgaard, N., T. Gjesteland, J. Stadsnes, P. H. Connell, and B. Carlson (2008), Pro-
484 duction altitude and time delays of the terrestrial gamma flashes: Revisiting the burst
485 and transient source experiment spectra, *Journal of Geophys. Res.*, *113*, A02,307, doi:
486 10.1029/2007JA012618.
- 487 Rodger, C. J., J. B. Brundell, R. H. Holzworth, and E. H. Lay (2009), Growing detection
488 efficiency of the world wide lightning location network, in *Conf. Proc. 1118, Coupling of*
489 *Thunderstorms and Lightning Discharges to Near-Earth Space*, edited by N. B. Crosby,
490 T.-Y. Huang, and M. J. Rycroft, pp. 15–20, AIP.
- 491 Smith, D. M., L. I. Lopez, R. P. Lin, and C. P. Barrington-Leigh (2005), Terrestrial
492 gamma-ray flashes observed up to 20 MeV, *Science*, *307*, 1085–1088.
- 493 Stanley, M. A., X.-M. Shao, D. M. Smith, L. I. Lopez, M. B. Pongratz, J. D.
494 Harlin, M. Stock, and A. Regan (2006), A link between terrestrial gamma-ray
495 flashes and intracloud lightning discharges, *Geophys. Res. Lett.*, *33*, L06,803, doi:
496 10.1029/2005GL025537.

⁴⁹⁷ Uman, M. A. (2001), *The Lightning Discharge*, Dover, 1249 Mineola, New York.

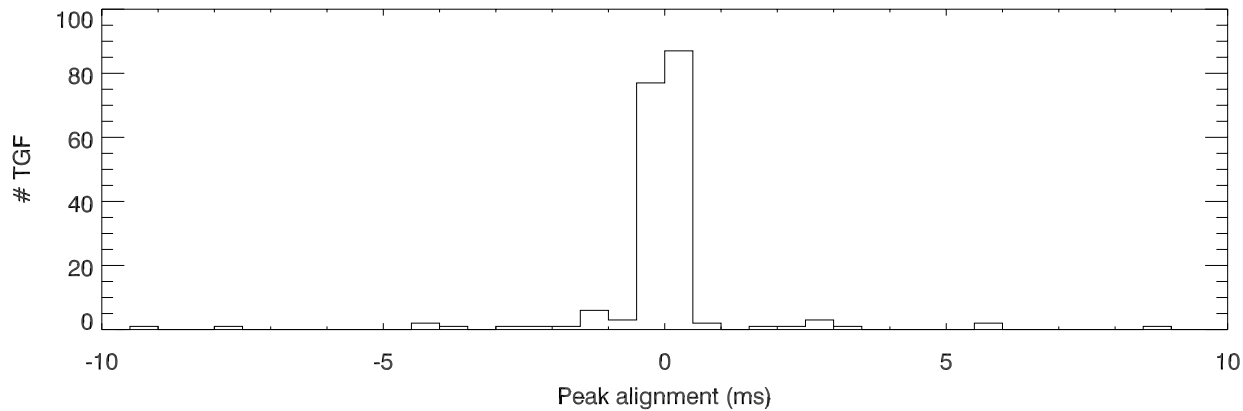
Figure 1. The top panel shows the offset distribution, in $500\ \mu\text{s}$ bins, of the TGF peak - the mid-point of the T_{50} interval (see text) - from 186 matched discharge times of group arrival measured by WWLLN. The lower plot zooms in on the region close to the TGF peak, containing most of the GBM-WWLLN matches. A $400\ \mu\text{s}$ interval centered on the TGF peak is used to define GBM-WWLLN simultaneity, and contains 154 of the associations.

Figure 2. The top panel shows the duration distribution in $50\ \mu\text{s}$ time bins of the 594 TGFs (salmon) with the subset of 154 TGFs having a match with a simultaneous WWLLN discharge shown in blue. We exclude likely electron-beam TGFs, which are generally much longer than the TGFs detected in gamma rays [Briggs *et al.*, 2011], and suppress for display purposes the two likely gamma-ray TGFs that have durations longer than 1 ms. In the bottom panel we rebin the distributions such that each time bin contains at least ten TGFs with associated simultaneous WWLLN discharges (the final, large, bin has no matches in the WWLLN data). The asterisks show the fraction of TGFs having WWLLN associations.

Figure 3. The top panel shows the duration distribution in $50\ \mu\text{s}$ time bins of the 594 TGFS (salmon) with the subset of 154 TGFS having a match with a simultaneous WWLLN discharge shown in blue. In the bottom panel we rebin the distributions such that each time bin contains at least ten TGFS with associated simultaneous WWLLN discharges. The asterisks show the fraction of TGFS having WWLLN associations. Similar to Figure 2 but with the T_{50} s measured for counts detected above 300 keV. Compared to Figure 2, the width of the T_{50} values is narrower and peaked at lower values for those TGFS with WWLLN associations. The number of very short TGFS with associations is also higher, and the number of longer TGFS with associations lower than when the T_{50} values are measured using the entire GBM energy range.

Figure 4. The estimated far-field VLF stroke energy of discharges measured by WWLLN in association with GBM-detected TGFS. *Hutchins et al.* [2012a] describe the procedure and reliability of measuring energies associated with WWLLN discharges. We include here 164 WWLLN discharges associated with TGFS for which energy measurements are available, and which have uncertainties lower than 70% of their value. The subset of non-simultaneous associations, which are farther than $\pm 200\ \mu\text{s}$ from the TGF peak, is shown in blue, the simultaneous associations in salmon. The non-simultaneous discharges have a significantly lower median energy (700 J) than the simultaneous discharges (3.1 kJ).

Number of TGFs as a function of time offset from WWLLN discharge



Alignment of Simultaneous TGF-WWLLN discharges

